

Four electron spin qubits with exchange interaction

H.W.L. Naus

*Quantum Technology, TNO, P.O. Box 155, 2600 AD Delft and QuTech,
Delft University of Technology, P.O. Box 5046, 2600 GA Delft, The Netherlands*
(Dated: March 18, 2022)

Four electron spin qubits in quantum dots are studied by means of an exchange interaction Hamiltonian. The time-independent Schrödinger equation is exactly analytically solved for the symmetric case, that is equal qubit frequencies and equal couplings. The spin system can be used as two data-qubits and two ancillas, thereby realizing a X and Z stabilizing circuit exploited in error correction and surface codes. The unitary evolution of corresponding stable states is calculated and consequences for error syndromes and fidelities are assessed. It is also shown that applying the evolution operator for a prescribed duration and subsequent measurement of the ancillas lead to a ‘verifiable’ two-qubit phase gate.

I. INTRODUCTION

In this study, we consider four electron spin qubits in quantum dots, which interact via an exchange Hamiltonian. Such a few-qubit system can serve as a simple stabilizing circuit exploited in error correction for fault-tolerant quantum computing. It also may be used as unit cell in a scalable many spin qubit quantum processor.

The reviews [1, 2], the thesis [3] and references therein introduce the basics of electron spins in quantum dots. The essential ingredient is the description of the low-energy physics of electrons in quantum dots by the exchange Hamiltonian, as argued in the seminal papers [4, 5]. The Heisenberg interaction for two confined electrons takes their Coulomb interaction and the Pauli exclusion principle effectively into account [6]. For electrons in quantum dots the possible tunneling process is included in [7, 8] by enlarging the 4D two-spin Hilbert space to a 6D space. In [7] the effective exchange interaction is rederived. Note that turning the tunneling on and off results in a time-dependent exchange coupling [4, 5]. Here we restrict ourselves to constant coupling; if it is taken to be equal for the interacting pairs of spin, the problem can be analytically exactly solved in the resonant case. Slightly different qubit frequencies may be taken into account perturbatively; we also present the explicit form of this perturbation.

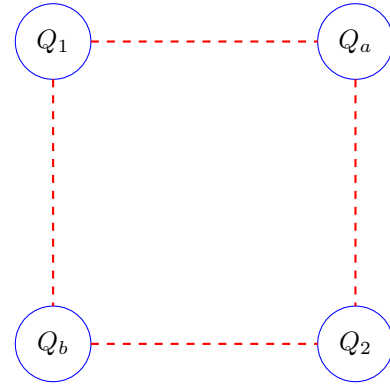
After solving the model Hamiltonian, we address the unitary evolution of the stable states used in the X and Z stabilizer circuits as introduced in [9]. Two qubits are considered as data qubits, whereas the other two are ancillas which are supposed to be measured. It is completely analogous to the recent analysis [10] of a coupled qubit-resonator system. Of course, the degrees of freedom and their dynamics are different. Therefore, we refer to [10] for further discussion and motivation of the followed approach. Our calculations have also demonstrated the possible implementation of phase gates for the data-qubits. They may be called ‘checkable’ or ‘verifiable’ gates because of concomitant ancilla measurements.

The outline of this paper is as follows. First, the exchange Hamiltonian of four interacting spins in a magnetic field is presented and solved for equal couplings and

frequencies. In section III, the general final state of the stabilizing circuit is rewritten in terms of singlet-triplet states. Subsequent unitary evolution and consequences for probabilities and fidelities are calculated in section IV. The next section V demonstrates the concept of verifiable gates. The final section presents conclusions.

II. FOUR INTERACTING SPINS

In order to analyze a simple stabilizer [9], we consider a spin system consisting out of two data qubits Q_1, Q_2 and two ancillas Q_a, Q_b . They are arranged as shown in the figure and only nearest neighbour interaction, indicated by the dashed red lines, is included.



The model Hamiltonian incorporating the exchange interaction is taken as

$$\begin{aligned}
 H &= H_0 + H_{\text{int}} \\
 &= \omega(S_z^{[1]} + S_z^{[2]}) + \tilde{\omega}(S_z^{[a]} + S_z^{[b]}) \\
 &\quad + \mathcal{J}(\vec{S}^{[1]} \cdot \vec{S}^{[a]} + \vec{S}^{[1]} \cdot \vec{S}^{[b]} + \vec{S}^{[2]} \cdot \vec{S}^{[a]} + \vec{S}^{[2]} \cdot \vec{S}^{[b]}) \\
 &= \omega(S_z^{[1]} + S_z^{[2]}) + \tilde{\omega}(S_z^{[a]} + S_z^{[b]}) \\
 &\quad + \mathcal{J}(\vec{S}^{[1]} + \vec{S}^{[2]}) \cdot (\vec{S}^{[a]} + \vec{S}^{[b]}).
 \end{aligned} \tag{1}$$

The ‘free’ Hamiltonian represents the energy of the electron spins in a homogeneous magnetic field in the z -direction. The electron spin operators are related to the

Pauli matrices

$$S_k = \frac{1}{2}\hbar\sigma_k, \quad k = x, y, z. \quad (2)$$

The constant \mathcal{J} is commonly known as the exchange interaction strength. After introducing the total four-spin operator \vec{J} as

$$\vec{J} = \vec{S}^{[1]} + \vec{S}^{[2]} + \vec{S}^{[a]} + \vec{S}^{[b]}, \quad (3)$$

the interaction Hamiltonian can be rewritten as

$$H_{\text{int}} = \frac{1}{2}\mathcal{J} \left(\vec{J}^2 - \left(\vec{S}^{[1]} + \vec{S}^{[2]} \right)^2 - \left(\vec{S}^{[a]} + \vec{S}^{[b]} \right)^2 \right). \quad (4)$$

It suggests the following construction of basis states. First, the data qubits are combined as singlet and triplet states; the same is done for the ancillas. Thus we have defined the respective two-qubit bases

$$\begin{aligned} &|S^{[12]}\rangle, |T_+^{[12]}\rangle, |T_0^{[12]}\rangle, |T_-^{[12]}\rangle \quad \text{and} \\ &|S^{[ab]}\rangle, |T_+^{[ab]}\rangle, |T_0^{[ab]}\rangle, |T_-^{[ab]}\rangle. \end{aligned} \quad (5)$$

Four-qubit basis states are now constructed by combining the two singlets, one singlet with a triplet yielding spin 1 ‘particles’ and the two triplets yielding a spin 0, a spin 1 and a spin 2 ‘particle’. We explicitly obtain for the singlets

$$|e_1\rangle = |S^{[12]}\rangle \otimes |S^{[ab]}\rangle \quad (j, m_j) = (0, 0) \quad (6)$$

and for the singlet triplet combinations

$$\begin{aligned} |e_2\rangle &= |S^{[12]}\rangle \otimes |T_+^{[ab]}\rangle & (j, m_j) &= (1, 1), \\ |e_3\rangle &= |S^{[12]}\rangle \otimes |T_0^{[ab]}\rangle & (j, m_j) &= (1, 0), \\ |e_4\rangle &= |S^{[12]}\rangle \otimes |T_-^{[ab]}\rangle & (j, m_j) &= (1, -1), \\ |e_5\rangle &= |T_+^{[12]}\rangle \otimes |S^{[ab]}\rangle & (j, m_j) &= (1, 1), \\ |e_6\rangle &= |T_0^{[12]}\rangle \otimes |S^{[ab]}\rangle & (j, m_j) &= (1, 0), \\ |e_7\rangle &= |T_-^{[12]}\rangle \otimes |S^{[ab]}\rangle & (j, m_j) &= (1, -1). \end{aligned} \quad (7)$$

We have indicated the quantum numbers of the total spin of the states. Combining the triplets yields [11] the scalar

$$|e_8\rangle = \frac{1}{3}\sqrt{3} \left\{ |T_+^{[12]}\rangle \otimes |T_-^{[ab]}\rangle - |T_0^{[12]}\rangle \otimes |T_0^{[ab]}\rangle + |T_-^{[12]}\rangle \otimes |T_+^{[ab]}\rangle \right\} \quad (j, m_j) = (0, 0) \quad (8)$$

and the spin 1 states

$$\begin{aligned} |e_9\rangle &= \frac{1}{2}\sqrt{2} \left\{ |T_+^{[12]}\rangle \otimes |T_0^{[ab]}\rangle - |T_0^{[12]}\rangle \otimes |T_+^{[ab]}\rangle \right\} & (j, m_j) &= (1, 1), \\ |e_{10}\rangle &= \frac{1}{2}\sqrt{2} \left\{ |T_+^{[12]}\rangle \otimes |T_-^{[ab]}\rangle - |T_-^{[12]}\rangle \otimes |T_+^{[ab]}\rangle \right\} & (j, m_j) &= (1, 0), \\ |e_{11}\rangle &= \frac{1}{2}\sqrt{2} \left\{ |T_0^{[12]}\rangle \otimes |T_-^{[ab]}\rangle - |T_-^{[12]}\rangle \otimes |T_0^{[ab]}\rangle \right\} & (j, m_j) &= (1, -1). \end{aligned} \quad (9)$$

Finally, we get the resulting spin 2 states

$$\begin{aligned} |e_{12}\rangle &= |T_+^{[12]}\rangle \otimes |T_+^{[ab]}\rangle & (j, m_j) &= (2, 2), \\ |e_{13}\rangle &= \frac{1}{2}\sqrt{2} \left\{ |T_+^{[12]}\rangle \otimes |T_0^{[ab]}\rangle + |T_0^{[12]}\rangle \otimes |T_+^{[ab]}\rangle \right\} & (j, m_j) &= (2, 1), \\ |e_{14}\rangle &= \frac{1}{6}\sqrt{6} \left\{ |T_+^{[12]}\rangle \otimes |T_-^{[ab]}\rangle + 2|T_0^{[12]}\rangle \otimes |T_0^{[ab]}\rangle + |T_-^{[12]}\rangle \otimes |T_+^{[ab]}\rangle \right\} & (j, m_j) &= (2, 0), \\ |e_{15}\rangle &= \frac{1}{2}\sqrt{2} \left\{ |T_0^{[12]}\rangle \otimes |T_-^{[ab]}\rangle + |T_-^{[12]}\rangle \otimes |T_0^{[ab]}\rangle \right\} & (j, m_j) &= (2, -1), \\ |e_{16}\rangle &= |T_-^{[12]}\rangle \otimes |T_-^{[ab]}\rangle & (j, m_j) &= (2, -2). \end{aligned} \quad (10)$$

If all qubits have the same frequency ω then the Hamiltonian H_0 reduces to

$$H_0 = \omega J_z, \quad (11)$$

i.e., proportional to the z -component of the total spin. Recall that we have presupposed equal exchange couplings from the onset. In this highly symmetric case, the complete Hamiltonian is diagonal in the defined basis $|e_k\rangle, k = 1, 2 \dots 16$. This is due to the fact the basis states are eigenstates of \vec{J}^2 and J_z but also of $(\vec{S}^{[1]} + \vec{S}^{[2]})^2$ and $(\vec{S}^{[a]} + \vec{S}^{[b]})^2$; these operators commute with H for $\omega = \tilde{\omega}$.

In other words, we have solved the time-independent Schrödinger equation for this case. The diagonal elements, these are the resonant eigenenergies, are found as $H_{kk} = h_k$, with

$$\begin{aligned} h_1 &= 0, & h_2 &= \hbar\omega, & h_3 &= 0, & h_4 &= -\hbar\omega, \\ h_5 &= \hbar\omega, & h_6 &= 0, & h_7 &= -\hbar\omega, & h_8 &= -2\hbar^2\mathcal{J}, \\ h_9 &= \hbar\omega - \hbar^2\mathcal{J}, & h_{10} &= -\hbar^2\mathcal{J}, & h_{11} &= -\hbar\omega - \hbar^2\mathcal{J}, \\ h_{12} &= 2\hbar\omega + \hbar^2\mathcal{J}, & h_{13} &= \hbar\omega + \hbar^2\mathcal{J}, & h_{14} &= \hbar^2\mathcal{J}, \\ h_{15} &= -\hbar\omega + \hbar^2\mathcal{J}, & h_{16} &= -2\hbar\omega + \hbar^2\mathcal{J}. \end{aligned} \quad (12)$$

This result can be verified by explicit calculation.

For nonequal frequencies $\omega, \tilde{\omega}$ the free Hamiltonian gets an additional term

$$H_0 = \omega J_z - \delta\omega(S_z^{[a]} + S_z^{[b]}), \quad (13)$$

with frequency difference $\delta\omega = \omega - \tilde{\omega}$. Some diagonal matrix elements get modified, $h_k \rightarrow \tilde{h}_k$:

$$\begin{aligned} \tilde{h}_2 &= \hbar(\omega - \delta\omega), & \tilde{h}_4 &= -\hbar(\omega - \delta\omega), \\ \tilde{h}_9 &= \hbar(\omega - \frac{1}{2}\delta\omega) - \hbar^2\mathcal{J}, & \tilde{h}_{11} &= -\hbar(\omega - \frac{1}{2}\delta\omega) - \hbar^2\mathcal{J}, \\ \tilde{h}_{12} &= 2\hbar\omega - \hbar\delta\omega + \hbar^2\mathcal{J}, & \tilde{h}_{13} &= \hbar(\omega - \frac{1}{2}\delta\omega) + \hbar^2\mathcal{J}, \\ \tilde{h}_{15} &= -(\hbar\omega - \frac{1}{2}\delta\omega) + \hbar^2\mathcal{J}, & \tilde{h}_{16} &= -2\hbar\omega + \hbar\delta\omega + \hbar^2\mathcal{J}. \end{aligned} \quad (14)$$

We furthermore obtain the following non-diagonal terms

$$\begin{aligned} H_{8-10} &= \frac{1}{3}\sqrt{6}\hbar\delta\omega, & H_{9-13} &= \frac{1}{2}\hbar\delta\omega, \\ H_{10-14} &= \frac{1}{3}\sqrt{3}\hbar\delta\omega, & H_{11-15} &= \frac{1}{2}\hbar\delta\omega \end{aligned} \quad (15)$$

and the identical transposed matrix elements. The consequence is mixing between the three states $|e_8\rangle, |e_{10}\rangle, |e_{14}\rangle$, between the two states $|e_9\rangle, |e_{13}\rangle$ and between $|e_{11}\rangle, |e_{15}\rangle$.

III. STABILIZING CIRCUIT

In analogy to [10], we analyze the stabilizing four-qubit circuit presented in [9], which is used in error correction surface codes. In particular, we study the consequences of unitary evolution governed by the Hamiltonian describing the interacting spins. To this end, we first rewrite the final state of the stabilizer circuit after putting in a general two-data qubit state with the ancillas in the ground state as given in [9, 10] as

$$\begin{aligned} |\psi\rangle &= A_+|\Phi^+\rangle \otimes |\downarrow\downarrow\rangle + B_+|\Psi^+\rangle \otimes |\downarrow\uparrow\rangle \\ &+ A_-|\Phi^-\rangle \otimes |\uparrow\downarrow\rangle + B_-|\Psi^-\rangle \otimes |\uparrow\uparrow\rangle \\ &= \frac{1}{2}\sqrt{2}A_+ (|T_+^{[12]}\rangle + |T_-^{[12]}\rangle) \otimes |\downarrow\downarrow\rangle \\ &+ B_+|T_0^{[12]}\rangle \otimes |\downarrow\uparrow\rangle - B_-|S^{[12]}\rangle \otimes |\uparrow\uparrow\rangle \\ &+ \frac{1}{2}\sqrt{2}A_- (|T_-^{[12]}\rangle - |T_+^{[12]}\rangle) \otimes |\uparrow\downarrow\rangle. \end{aligned} \quad (16)$$

Here we have introduced the data-qubit Bell states

$$\begin{aligned} |\Phi^\pm\rangle &= \frac{1}{2}(|\downarrow\downarrow\rangle \pm |\uparrow\uparrow\rangle), \\ |\Psi^\pm\rangle &= \frac{1}{2}(|\downarrow\uparrow\rangle \pm |\uparrow\downarrow\rangle). \end{aligned} \quad (17)$$

Expressing the ancilla states in singlet-triplet states yields

$$\begin{aligned} |\psi\rangle &= \frac{1}{2}\sqrt{2}A_+ (|T_+^{[12]}\rangle + |T_-^{[12]}\rangle) \otimes |T_-^{[ab]}\rangle \\ &+ \frac{1}{2}\sqrt{2}B_+|T_0^{[12]}\rangle \otimes (|T_0^{[ab]}\rangle - |S^{[ab]}\rangle) \\ &+ \frac{1}{2}A_- (|T_-^{[12]}\rangle - |T_+^{[12]}\rangle) \otimes (|S^{[ab]}\rangle + |T_0^{[ab]}\rangle) \\ &- B_-|S^{[12]}\rangle \otimes |T_+^{[ab]}\rangle. \end{aligned} \quad (18)$$

Measuring the ancillas projects this state onto the product of a data-qubit state and the ancilla state corresponding to the obtained result. Re-inserting such a state into

the circuit, including re-initialization of the ancillas in the ground state, yields the same state. It means that the measurement result is again found with probability one. The state is therefore called stable. Unitary evolution, however, may reduce the probability to obtain the desired result. This would be interpreted as an error detection [9, 10]. Apart from the changed, that is non-zero and not one probabilities, the fidelity of the state after some elapsed time is a measure for the unwanted effects of evolution.

IV. UNITARY EVOLUTION AND ITS CONSEQUENCES

Here we consider the unitary evolution for the case of zero detuning, *i.e.*, $\omega = \tilde{\omega}$. As shown above, it implies that the introduced basis states $|e_k\rangle$ are the eigenstates of the Hamiltonian with eigenenergies $E_k = h_k$. The evolution operator therefore follows as

$$U(t) = \sum_{k=1}^{16} \exp(-iE_k t) |e_k\rangle \langle e_k|, \quad (19)$$

where we have adopted $\hbar = 1$. The ancilla measurement operators are given by

$$\begin{aligned} P_{\downarrow\downarrow} &= \mathcal{I}^{12} \otimes |\downarrow\downarrow\rangle \langle \downarrow\downarrow| = \mathcal{I}^{12} \otimes |T_-^{[ab]}\rangle \langle T_-^{[ab]}|, \\ P_{\downarrow\uparrow} &= \mathcal{I}^{12} \otimes |\downarrow\uparrow\rangle \langle \downarrow\uparrow| \\ &= \frac{1}{2}\mathcal{I}^{12} \otimes (|T_0^{[ab]}\rangle - |S^{[ab]}\rangle)(\langle T_0^{[ab]}| - \langle S^{[ab]}|), \\ P_{\uparrow\downarrow} &= \mathcal{I}^{12} \otimes |\uparrow\downarrow\rangle \langle \uparrow\downarrow| \\ &= \frac{1}{2}\mathcal{I}^{12} \otimes (|T_0^{[ab]}\rangle + |S^{[ab]}\rangle)(\langle T_0^{[ab]}| + \langle S^{[ab]}|), \\ P_{\uparrow\uparrow} &= \mathcal{I}^{12} \otimes |\uparrow\uparrow\rangle \langle \uparrow\uparrow| = \mathcal{I}^{12} \otimes |T_+^{[ab]}\rangle \langle T_+^{[ab]}|. \end{aligned} \quad (20)$$

In the following we calculate the consequences of evolution for the four different ‘initial’ states. We denote them as in [9, 10]. The shown numerical results are calculated with the parameter values: $\omega = 18.5$ GHz and $\mathcal{J} = 80$ MHz, $\mathcal{J} = 800$ MHz.

A. Bell state $|\Phi^+\rangle$

The corresponding four qubit state $|\phi^+\rangle$ follows from (18) by taking $A_+ = 1, A_- = B_+ = B_- = 0$. We expand this state in terms of the basis states and find

$$|\phi^+\rangle = \frac{1}{6}\sqrt{6}|e_8\rangle + \frac{1}{2}|e_{10}\rangle + \frac{1}{6}\sqrt{3}|e_{14}\rangle + \frac{1}{2}\sqrt{2}|e_{16}\rangle. \quad (21)$$

Its time evolution is easily obtained as

$$\begin{aligned} |\phi^+(t)\rangle &= \frac{1}{6}\sqrt{6}e^{-iE_8 t}|e_8\rangle + \frac{1}{2}e^{-iE_{10} t}|e_{10}\rangle \\ &+ \frac{1}{6}\sqrt{3}e^{-iE_{14} t}|e_{14}\rangle + \frac{1}{2}\sqrt{2}e^{-iE_{16} t}|e_{16}\rangle. \end{aligned} \quad (22)$$

By means of (20) we then get

$$P_{\downarrow\downarrow}|\phi^+(t)\rangle = \frac{1}{2}\sqrt{2} \left\{ \alpha(t)|T_+^{[12]}\rangle + e^{-iE_{16} t}|T_-^{[12]}\rangle \right\} \otimes |T_-^{[ab]}\rangle, \quad (23)$$

where we have defined

$$\alpha(t) = \frac{1}{3}e^{-iE_8t} + \frac{1}{2}e^{-iE_{10}t} + \frac{1}{6}e^{-iE_{14}t}. \quad (24)$$

The probability of indeed measuring $\downarrow\downarrow$ therefore reads

$$p_{\downarrow\downarrow} = \frac{1}{2} (1 + \alpha^*(t)\alpha(t)). \quad (25)$$

After factoring out the ancillas we obtain as normalized final two-qubit state

$$|\Phi(t)\rangle = \frac{1}{\sqrt{2p_{\downarrow\downarrow}}} \left\{ \alpha(t)|T_+^{[12]}\rangle + e^{-iE_{16}t}|T_-^{[12]}\rangle \right\}. \quad (26)$$

This leads to the fidelity

$$F = |\langle\Phi^+|\Phi(t)\rangle| \quad (27)$$

$$= \frac{1}{2} \left[1 + \frac{1}{1 + \alpha^*(t)\alpha(t)} (\alpha(t)e^{iE_{16}t} + \alpha^*(t)e^{-iE_{16}t}) \right]^{1/2}.$$

It turns out that is a very fast oscillating quantity, governed by the frequency 2ω . This less interesting ‘free’ evolution can be eliminated exploiting the rotating frame, cf. [10]. The fidelity in this rotating frame is obtained by replacing E_{16} by \mathcal{J} in (28) and is depicted in figure (1) for two values of the exchange constant \mathcal{J} . Changing

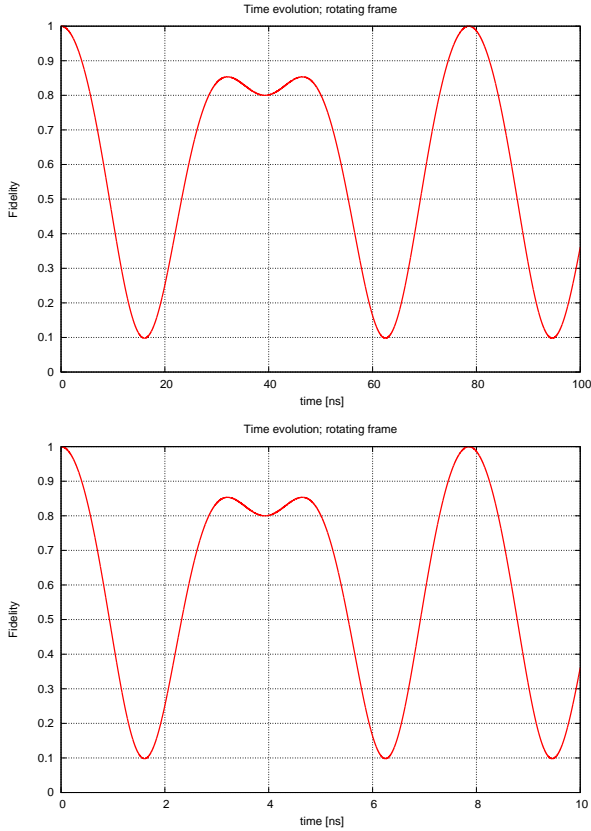


FIG. 1. Fidelities: top $\mathcal{J} = 80$ MHz; low $\mathcal{J} = 800$ MHz; note the timescales.

the vales of \mathcal{J} merely changes the timescale: stronger coupling causes a faster decrease in fidelity.

Analogous computations yield the probabilities to obtain the other possible measurement results:

$$p_{\downarrow\uparrow} = p_{\uparrow\downarrow} = \frac{1}{18} [1 - \cos \{(E_{14} - E_8)t\}] \quad (28)$$

and

$$p_{\uparrow\uparrow} = \beta^*(t)\beta(t), \quad (29)$$

with

$$\beta(t) = \frac{1}{2}\sqrt{2} \left(\frac{1}{3}e^{-iE_8t} - \frac{1}{2}e^{-iE_{10}t} + \frac{1}{6}e^{-iE_{14}t} \right). \quad (30)$$

Note that the sum of the probabilities indeed is equal to one for all t . They are shown in figure (2). Again we

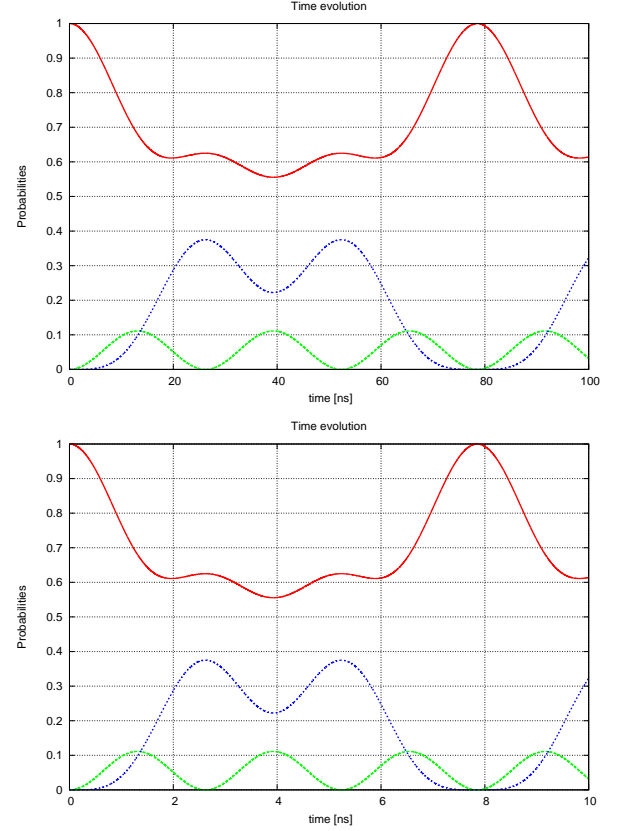


FIG. 2. Probabilities: $p_{\downarrow\downarrow}$ red, $p_{\downarrow\uparrow} = p_{\uparrow\downarrow}$ green, $p_{\uparrow\uparrow}$ blue; top $\mathcal{J} = 80$ MHz; low $\mathcal{J} = 800$ MHz; note the timescales.

note that altering the value of \mathcal{J} changes the timescale; in this case for the varying probabilities.

B. Bell state $|\Psi^+\rangle$

We repeat these computations for the other Bell states as well. First, we consider $|\Psi^+\rangle$ which corresponds to $B_+ = 1, A_+ = A_- = B_- = 0$ in (18). Initial and time-evolved state follow respectively as

$$|\psi^+\rangle = -\frac{1}{2}\sqrt{2}|e_6\rangle - \frac{1}{6}\sqrt{6}|e_8\rangle + \frac{1}{3}\sqrt{3}|e_{14}\rangle \quad (31)$$

and

$$|\psi^+(t)\rangle = -\frac{1}{2}\sqrt{2}e^{-iE_6t}|e_6\rangle - \frac{1}{6}\sqrt{6}e^{-iE_8t}|e_8\rangle + \frac{1}{3}\sqrt{3}e^{-iE_{14}t}|e_{14}\rangle. \quad (32)$$

Using the measurement operator corresponding to the ‘correct result’ yields

$$P_{\downarrow\uparrow}|\psi^+(t)\rangle = \gamma(t)|T_0^{[12]}\rangle \otimes (|T_0^{[ab]}\rangle - |S^{[ab]}\rangle), \quad (33)$$

a product state, with time dependence

$$\gamma(t) = \frac{1}{2}e^{-iE_6t} + \frac{1}{6}e^{-iE_8t} + \frac{1}{3}e^{-iE_{14}t}. \quad (34)$$

This leads to the probability

$$p_{\downarrow\uparrow} = \gamma^*(t)\gamma(t). \quad (35)$$

The resulting two-qubit state

$$|\Psi(t)\rangle = \frac{\gamma(t)}{\sqrt{p_{\downarrow\uparrow}}} |T_0^{[12]}\rangle \quad (36)$$

has fidelity one with respect to the target state $|\Psi^+\rangle$.

The probabilities for obtaining the results which would be interpreted as error detection follow as

$$p_{\downarrow\downarrow} = p_{\uparrow\uparrow} = \frac{1}{9} [1 - \cos \{(E_{14} - E_8)t\}] \quad (37)$$

and

$$p_{\uparrow\downarrow} = \mu^*(t)\mu(t), \quad (38)$$

with

$$\mu(t) = -\frac{1}{2}e^{-iE_6t} + \frac{1}{6}e^{-iE_8t} + \frac{1}{3}e^{-iE_{14}t}. \quad (39)$$

The various probabilities, indeed adding up to one, are shown in figure (3). Once more, we see time-scaling with the coupling strength.

C. Bell state $|\Phi^-\rangle$

Next, we take $A_- = 1, A_+ = B_- = B_+ = 0$ in (18) corresponding to the two-qubit state $|\Phi^-\rangle$. We immediately proceed to the state after time-evolution:

$$|\phi^-(t)\rangle = -\frac{1}{2}e^{-iE_5t}|e_5\rangle + \frac{1}{2}e^{-iE_7t}|e_7\rangle - \frac{1}{4}\sqrt{2}e^{-iE_9t}|e_9\rangle - \frac{1}{4}\sqrt{2}e^{-iE_{11}t}|e_{11}\rangle - \frac{1}{4}\sqrt{2}e^{-iE_{13}t}|e_{13}\rangle + \frac{1}{4}\sqrt{2}e^{-iE_{14}t}|e_{14}\rangle. \quad (40)$$

Operating with the appropriate measurement operator for the ‘correct result’ gives

$$P_{\uparrow\downarrow}|\phi^-(t)\rangle = -\frac{1}{8}\sqrt{2} \left\{ \chi_+(t)|T_+^{[12]}\rangle - \chi_-(t)|T_-^{[12]}\rangle \right\} \otimes \left(|T_0^{[ab]}\rangle + |S^{[ab]}\rangle \right), \quad (41)$$

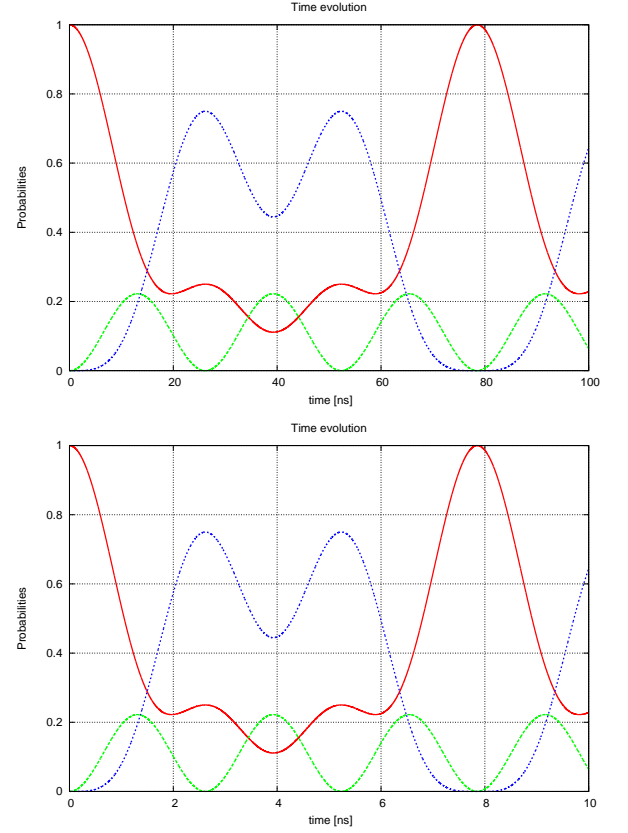


FIG. 3. Probabilities: $p_{\downarrow\uparrow}$ red, $p_{\uparrow\uparrow} = p_{\downarrow\downarrow}$ green, $p_{\uparrow\downarrow}$ blue; top $J = 80$ MHz; low $J = 800$ MHz; note the timescales.

with the functions

$$\begin{aligned} \chi_+(t) &= 2e^{-iE_5t} + e^{-iE_9t} + e^{-iE_{13}t}, \\ \chi_-(t) &= 2e^{-iE_7t} + e^{-iE_{11}t} + e^{-iE_{15}t}. \end{aligned} \quad (42)$$

The probability to get the measurement result \uparrow, \downarrow follows as

$$p_{\uparrow\downarrow} = \frac{1}{32} (\chi_+^*(t)\chi_+(t) + \chi_-^*(t)\chi_-(t)). \quad (43)$$

After factoring out the ancilla states we obtain for the corresponding fidelity

$$F = \frac{1}{8} [(\chi_+(t) + \chi_-(t)) (\chi_+^*(t) + \chi_-^*(t)) / p_{\uparrow\downarrow}]^{1/2}. \quad (44)$$

This fidelity also oscillates very fast. This is a result of the interference terms $\chi_+^*\chi_-$ and $\chi_-^*\chi_+$ which have a frequency of 2ω . In the rotating frame of the qubits it vanishes. The resulting fidelity in this frame is equal one for all times since in the rotating frame

$$\chi_{\pm}(t) \rightarrow \tilde{\chi}_{\pm}(t) = e^{\pm i\omega t} \chi_{\pm}(t) \quad (45)$$

and $\tilde{\chi}_+(t) = \tilde{\chi}_-(t)$. As a consequence, we obtain

$$F = \frac{1}{8} [64p_{\uparrow\downarrow}/p_{\uparrow\downarrow}]^{1/2} = 1, \quad (46)$$

which may be somewhat surprising.

The other, ‘error detection’ probabilities can be calculated analogously. We get the results

$$\begin{aligned} p_{\downarrow\downarrow} &= \frac{1}{8} [1 - \cos \{(E_{15} - E_{11})t\}], \\ p_{\uparrow\uparrow} &= \frac{1}{8} [1 - \cos \{(E_{13} - E_9)t\}], \\ p_{\downarrow\uparrow} &= \frac{1}{32} (\nu_+^*(t)\nu_+(t) + \nu_-^*(t)\nu_-(t)), \end{aligned} \quad (47)$$

where we have defined

$$\begin{aligned} \nu_+(t) &= 2e^{-iE_5t} - e^{-iE_9t} - e^{-iE_{13}t}, \\ \nu_-(t) &= 2e^{-iE_7t} - e^{-iE_{11}t} - e^{-iE_{15}t}. \end{aligned} \quad (48)$$

From the eigenenergies (12) it becomes clear that $p_{\downarrow\downarrow} = p_{\uparrow\uparrow}$. Figure (4) depicts the calculated probabilities. We again get time-scaling with the coupling strength.

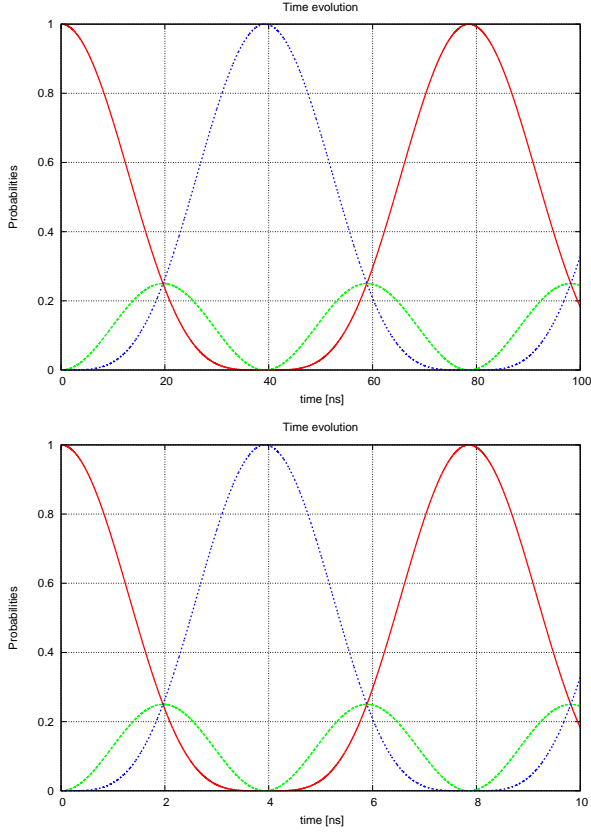


FIG. 4. Probabilities: $p_{\downarrow\downarrow}$ red, $p_{\uparrow\uparrow} = p_{\downarrow\downarrow}$ green, $p_{\downarrow\uparrow}$ blue; top $\mathcal{J} = 80$ MHz; low $\mathcal{J} = 800$ MHz; note the timescales.

D. Bell state $|\Psi^-\rangle$

This last case corresponds to $B_- = 1, A_+ = A_- = B_+ = 0$ in (18); it actually is the simplest one because the initial four qubit state equals a basis state. Explicitly we obtain

$$\begin{aligned} |\psi_-\rangle &= -|e_2\rangle, \\ |\psi_-(t)\rangle &= -e^{-iE_2t}|e_2\rangle, \\ P_{\uparrow\uparrow}|\psi_-(t)\rangle &= -e^{-iE_2t}|S^{[12]}\rangle \otimes |T_+^{[ab]}\rangle \end{aligned} \quad (49)$$

and the concomitant trivial probabilities

$$p_{\uparrow\uparrow} = 1, \quad p_{\uparrow\downarrow} = p_{\downarrow\uparrow} = p_{\downarrow\downarrow} = 0. \quad (50)$$

After factoring out the ancillas state, the two-qubit state is -up to a phase- equal to the target state. As a consequence, the fidelity is equal to one. The unitary evolution has no negative impact on the ideal probabilities and fidelity for this particular Bell state.

V. QUANTUM GATES BY UNITARY EVOLUTION

The obtained results show that the probabilities which were initially one, first decrease but after a time \tilde{t} again become equal to one. For the Bell state $|\Phi^-\rangle$, we note that for $t = \tilde{t}/2$ the up-down probability (initially one) becomes zero, whereas the down-up probability equals one. This opens the possibility for two-qubit gates, that is an operation on the data qubits, which can be verified by measuring the ancillas without affecting the state of the data qubits. The time \tilde{t} follows from

$$\mathcal{J}\tilde{t} = 2\pi \quad \text{as} \quad \tilde{t} = \frac{2\pi}{\mathcal{J}}. \quad (51)$$

In order to address two-qubit gates in the four-qubit system we continue the analysis started above. To this end, we also need the computational basis. For two qubits we define the basis states $|c_k\rangle, k = 1, 2, 3, 4$ as the common computational states

$$|c_1\rangle = |\downarrow\downarrow\rangle, |c_2\rangle = |\downarrow\uparrow\rangle, |c_3\rangle = |\uparrow\downarrow\rangle, |c_4\rangle = |\uparrow\uparrow\rangle. \quad (52)$$

The computational states for four qubits are the product states

$$|c_{kl}\rangle = |c_k^{[12]}\rangle \otimes |c_l^{[ab]}\rangle, \quad k, l = 1, 2, 3, 4. \quad (53)$$

We relabel the ancilla measurement operators (20) also as P_l and rewrite these as

$$P_l^{[ab]} = \mathcal{I}^{12} \otimes |c_l^{[ab]}\rangle \langle c_l^{[ab]}| = \sum_{j=1}^4 |c_{jl}\rangle \langle c_{jl}|. \quad (54)$$

The initial state is assumed to be the product state of a computational basis state of the ancillas, say $|c_n^{[ab]}\rangle$ with fixed n and a general two-data qubit state:

$$|\psi_0\rangle = \left\{ \sum_{m=1}^4 \alpha_m |c_m^{[12]}\rangle \right\} \otimes |c_n^{[ab]}\rangle = \sum_{m=1}^4 \alpha_m |c_{mn}\rangle. \quad (55)$$

After unitary evolution governed by the operator (19), the state is given by

$$|\psi(t)\rangle = \sum_{k=1}^{16} \sum_{m=1}^4 \alpha_m \langle e_k | c_{mn} \rangle e^{-iE_k t} |e_k\rangle. \quad (56)$$

Applying the ancilla measurement operator $P_l^{[ab]}$ to this state yields

$$\begin{aligned} P_l^{[ab]}|\psi(t)\rangle &= \sum_{j=1}^4 \sum_{m=1}^4 \alpha_m W_{jl-mn}(t) |c_{jl}\rangle \\ &= \left\{ \sum_{j=1}^4 \sum_{m=1}^4 \alpha_m W_{jl-mn}(t) |c_j^{[12]}\rangle \right\} \otimes |c_l^{[ab]}\rangle, \end{aligned} \quad (57)$$

where we have defined

$$W_{jl-mn}(t) = \sum_{k=1}^{16} \langle e_k | c_{mn} \rangle \langle c_{jl} | e_k \rangle e^{-iE_k t}. \quad (58)$$

Since the coefficients $\langle e_k | c_{mn} \rangle$ are real, W is symmetric: $W_{jl-mn}(t) = W_{mn-jl}(t)$. The measurement probabilities for obtaining the result l follow as

$$p_{ln}(t) = \sum_{m=1}^4 \sum_{m'=1}^4 \sum_{j=1}^4 \alpha_{m'}^* \alpha_m W_{jl-m'n}^*(t) W_{jl-mn}(t), \quad (59)$$

where we have explicitly indicated the dependence on the initial ancillas state. Note the implicit dependence on the initial data qubit states. The corresponding amputated and normalized final data qubit state is obtained as

$$\begin{aligned} |\psi_{ln}^{[12]}(t)\rangle &= \frac{1}{\sqrt{p_{ln}}} \sum_{j=1}^4 \sum_{m=1}^4 \alpha_m W_{jl-mn}(t) |c_j^{[12]}\rangle \\ &= \sum_{j=1}^4 \beta_j^{[ln]}(t) |c_j^{[12]}\rangle, \end{aligned} \quad (60)$$

with the functions

$$\beta_j^{[ln]}(t) = \frac{1}{\sqrt{p_{ln}}} \sum_{m=1}^4 \alpha_m W_{jl-mn}(t). \quad (61)$$

Comparison of this final state and the initial one (55) suggest a linear relation between these states. Because of the abovementioned dependence of the probabilities on the coefficients α_m this is, however, in general not true. The dependence only vanishes for zero probability which is not interesting and for the relevant case of probability one. If for an instant of time \tilde{t} and a specific combination of l, n

$$\sum_{j=1}^4 W_{jl-m'n}^*(\tilde{t}) W_{jl-mn}(\tilde{t}) = \delta_{mm'}, \quad (62)$$

the probability becomes one

$$p_{ln}(\tilde{t}) = \sum_{m=1}^4 \sum_{m'=1}^4 \alpha_{m'}^* \alpha_m \delta_{mm'} = \sum_{m=1}^4 \alpha_m^* \alpha_m = 1. \quad (63)$$

In fact, in the numerical implementation described below, we have found that the specific l, n combinations are $l =$

n . Thus the latter two equations actually read

$$\sum_{j=1}^4 W_{jl-m'n}^*(\tilde{t}) W_{jl-mn}(\tilde{t}) = \delta_{mm'} \delta_{ln}, \quad (64)$$

and

$$p_{ln}(\tilde{t}) = \delta_{ln} \sum_{m=1}^4 \sum_{m'=1}^4 \alpha_{m'}^* \alpha_m \delta_{mm'} = \delta_{ln} \sum_{m=1}^4 \alpha_m^* \alpha_m = \delta_{ln}. \quad (65)$$

It indeed implies that the coefficients $\beta_j^{[nn]}(\tilde{t})$ depend linearly on the initial ones α_m . Consequently, we obtain a final two-qubit state which follows as a gate operation on the initial one

$$\begin{aligned} |\psi_{nn}^{[12]}(\tilde{t})\rangle &= \sum_{j=1}^4 \beta_j^{[nn]}(\tilde{t}) |c_j^{[12]}\rangle \\ &= \sum_{j=1}^4 \sum_{m=1}^4 \alpha_m W_{jn-mn}(\tilde{t}) |c_j^{[12]}\rangle. \end{aligned} \quad (66)$$

In matrix form, the gate is explicitly given by

$$\beta_j^{[nn]}(\tilde{t}) = \sum_{m=1}^4 W_{jn-mn}(\tilde{t}) \alpha_m. \quad (67)$$

Unitarity of the gate, or matrix, is guaranteed by the constraints (62,64). Note that, for an arbitrary initial data qubit state, the probability only becomes one for obtaining the *same* ancilla spin values as initialized. In situations where the data qubits are initialized in a specific computational state, other measurement results, e.g. $\downarrow\uparrow$ instead of $\uparrow\downarrow$, with probability one also have appeared. It does not simultaneously happen, however, for all four initial computational data qubit states and, consequently, no unitary operation is effectuated.

In the way described above, four unitary gates are in principle obtained by evolution and projection at $t = \tilde{t}$:

$$U_{jm}^n(\tilde{t}) = W_{jn-mn}(\tilde{t}), \quad n = 1, 2, 3, 4. \quad (68)$$

It will further be analyzed numerically as well as analytically; these methods have turned out to be complementary for obtaining the results.

A. Implementation

We have implemented the formalism in a computer program. To compute the quantities $W_{jl-mn}(t)$, all the necessary ingredients have been obtained analytically. These are the eigenstates $|e_k\rangle$ and the concomitant energy eigenvalues E_k presented in section II. Additionally, the basis transformation $\langle e_k | c_{mn} \rangle$ is needed. Since the eigenstates are expressed in singlet-triplet basis states - for data and ancilla qubits - it can be computed using the transformation between singlet-triplet and computational basis. Next the measurement probabilities (59) are

calculated for given initial data qubit state, *i.e.*, given coefficients α_m . They can be chosen by hand or randomly generated by a random-number generator for a given probability density function. We have chosen a uniform distribution around zero for real as well as imaginary parts. Of course, the state has then to be normalized. The resulting measurement probabilities for all l, n combinations are plotted as a function of time and the instant of time where a probability becomes one is identified. Indeed we find that for $l = n$ this instant of time is given by $\tilde{t} = \frac{2\pi}{\mathcal{J}}$. Figure (5) shows the measurement probabilities for $n = 1$ and $n = 2$ and all $l = 1, 2, 3, 4$. It explicitly illustrates the already mentioned results. The initial data qubit state is randomly selected in this example.

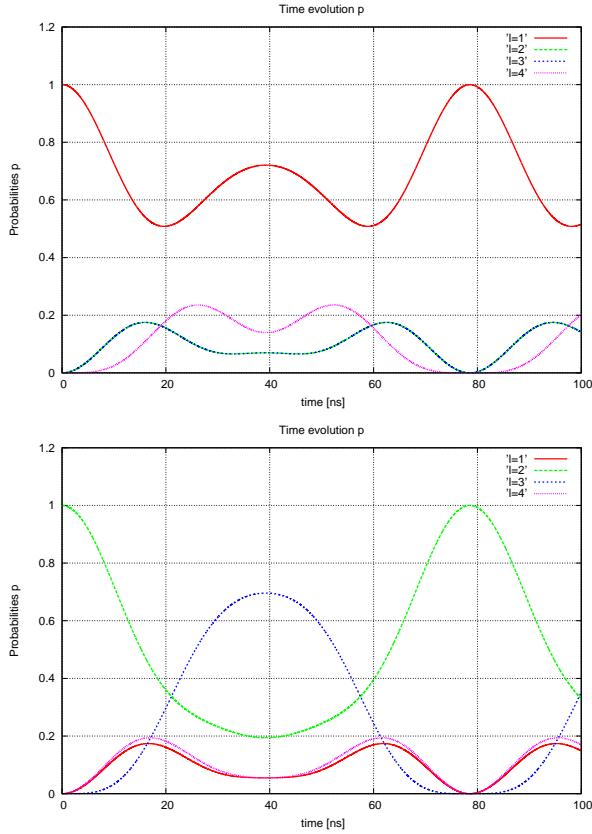


FIG. 5. Probabilities: $\mathcal{J} = 80$ MHz; top $n = 1$, low $n = 2$

The resulting gates explicitly read

$$U^1 = \begin{pmatrix} e^{\frac{4\pi i \omega}{\mathcal{J}}} & 0 & 0 & 0 \\ 0 & e^{\frac{2\pi i \omega}{\mathcal{J}}} & 0 & 0 \\ 0 & 0 & e^{\frac{2\pi i \omega}{\mathcal{J}}} & 0 \\ 0 & 0 & 0 & 1 \end{pmatrix},$$

$$U^2 = e^{-\frac{2\pi i \omega}{\mathcal{J}}} U^1, \quad U^3 = e^{-\frac{2\pi i \omega}{\mathcal{J}}} U^2,$$

$$U^4 = e^{-\frac{2\pi i \omega}{\mathcal{J}}} U^3. \quad (69)$$

These are four, phase-equivalent phase gates.

B. Analytical construction

With some effort, these gates can be obtained analytically as well. The initial state is completely specified as a product state of a computational data qubit state and a computational ancilla qubit state. It is rewritten in terms of eigenstates of the Hamiltonian in order to construct the time-evolved state. Next the time is identified upon a measurement yields a result with probability one and the resulting two-data-qubit state is identified. Let us explicitly demonstrate this for the initial state

$$|\phi_0\rangle = |\downarrow\downarrow\rangle \otimes |\downarrow\uparrow\rangle, \quad (70)$$

which reads in terms of singlet-triplet basis states as

$$|\phi_0\rangle = \frac{1}{2}\sqrt{2}|T_-^{[12]}\rangle \left(|T_0^{[ab]}\rangle - |S^{[ab]}\rangle \right). \quad (71)$$

Rewriting it as a linear combination of eigenstates yields

$$|\phi_0\rangle = -\frac{1}{2} \left(|e_{11}\rangle - |e_{15}\rangle + \sqrt{2}|e_7\rangle \right). \quad (72)$$

As a consequence, after time evolution we get

$$|\phi(t)\rangle = -\frac{1}{2} \left(e^{-iE_{11}t}|e_{11}\rangle - e^{-iE_{15}t}|e_{15}\rangle + \sqrt{2}e^{iE_7t}|e_7\rangle \right). \quad (73)$$

Now it is readily checked that

$$\begin{aligned} |\phi(\tilde{t})\rangle &= -\frac{1}{2} \left(e^{i\omega\tilde{t}}|e_{11}\rangle - e^{i\omega\tilde{t}}|e_{15}\rangle + \sqrt{2}e^{i\omega\tilde{t}}|e_7\rangle \right) \\ &= e^{i\omega\tilde{t}}|\phi_0\rangle, \end{aligned} \quad (74)$$

which implies $p_{\downarrow,\uparrow} = 1$ for $t = \tilde{t}$. Thus the resulting change in the data two qubit state can be identified as

$$|\downarrow\downarrow\rangle \rightarrow e^{\frac{2\pi i \omega}{\mathcal{J}}} |\downarrow\downarrow\rangle = U_{11}^2 |\downarrow\downarrow\rangle. \quad (75)$$

At this point it also follows that $U_{1m}^2 = 0$ for $m = 2, 3, 4$. In this way, all four gates given in (69) can be constructed.

C. Universality

Naturally the question arises whether the U^k are universal gates. Since they are phase-equivalent, we just consider U^2 . The unitary matrix U^2 acts non-trivially on two vector components because it is diagonal with two elements equal to one. Consequently, it is a two-level unitary matrix [12]. Any unitary matrix can be decomposed in terms of two-level unitary matrices. In [12], this fact is used to prove universality of CNOT-gates and single qubit gates. The reasoning is that with these gates one may construct an arbitrary two-level unitary operation and these, in turn, can be used to build any unitary operation. However, generally a number of two-level unitary matrices is necessary. Thus the fact that U^2 is two-level unitary operation does *not* imply that U^2 (and single

qubit gates) is indeed sufficient universal for quantum computing.

It is actually easy to see that U^2 can be written as a product of single qubit rotations:

$$R_z^{[1]}(\beta) \otimes R_z^{[2]}(\beta) = \begin{pmatrix} e^{-i\beta} & 0 & 0 & 0 \\ 0 & 1 & 0 & 0 \\ 0 & 0 & 1 & 0 \\ 0 & 0 & 0 & e^{i\beta} \end{pmatrix}, \quad (76)$$

which is equal to U^2 for $\beta = -2\pi i\omega/\mathcal{J}$.

Nevertheless we believe it to be elucidating to demonstrate that U^2 can be written in terms of CNOT-like operations and a controlled single qubit rotation (as is done in [12] for a different example). Instead of the standard CNOT we need the controlled operation with the NOT gate being performed on the second qubit, conditional on the first qubit being in the ground state, cf. [12] Figure (4.11). Denoting this gate C^0 , we explicitly have in the computational basis

$$C^0 = \begin{pmatrix} 0 & 1 & 0 & 0 \\ 1 & 0 & 0 & 0 \\ 0 & 0 & 1 & 0 \\ 0 & 0 & 0 & 1 \end{pmatrix}. \quad (77)$$

Next we use the single qubit operation \tilde{U} which is applied to the first qubit conditional on the second qubit (being excited); the 2-qubit operation is denoted by $C_{\tilde{U}}$. These matrices read

$$\tilde{U} = \begin{pmatrix} e^{\frac{2\pi i\omega}{\mathcal{J}}} & 0 \\ 0 & e^{-\frac{2\pi i\omega}{\mathcal{J}}} \end{pmatrix}, \quad C_{\tilde{U}} = \begin{pmatrix} 1 & 0 & 0 & 0 \\ 0 & e^{\frac{2\pi i\omega}{\mathcal{J}}} & 0 & 0 \\ 0 & 0 & 1 & 0 \\ 0 & 0 & 0 & e^{-\frac{2\pi i\omega}{\mathcal{J}}} \end{pmatrix}. \quad (78)$$

By matrix multiplication it can easily be verified that

$$U^2 = C^0 C_{\tilde{U}} C^0, \quad (79)$$

thereby having achieved the desired decomposition. Note that $C_{\tilde{U}}$ is a controlled rotation around z -axis.

D. Discussion

The ancilla measurement at $t = \tilde{t}$ should yield with probability one the same spin values for the ancillas as in the initialization. Therefore it serves as a check whether the gate operation on data qubits has been performed correctly without affecting this data qubit state. A different ancilla measurement result indicates an error. In this way ‘verifiable’ phase gates are effectuated. In practice, an error can nevertheless not be excluded.

In an actual application, it is of course not necessary to measure the ancillas at $t = \tilde{t}$. At that moment, the complete four-qubit state is a product state of the state of the ancillas and a two data-qubit state which is predictable. Moreover, its evolution starting from an arbitrary state

is described by a unitary phase gate. Switching off the interaction \mathcal{J} at $t = \tilde{t}$ ensures that data qubits and ancillas then remain decoupled and the subsequent dynamics is only governed by free evolution.

Above, we have already addressed the topic of universality of the constructed U^k gates. For universal quantum computing, we would need to express the CNOT-gate or the CZ gate in terms of the considered gate and single qubit operations. Since the U^2 phase gate can be written as the product of two single qubit rotations, this is not possible. Nevertheless, the found gates may be applicable in quantum computation if complemented by additional operations. The controlled Z -rotation $C_{\tilde{U}}$ can actually be useful in the quantum Fourier transformation.

Suppose one measures the ancillas at another moment where there are generally four non-zero probabilities for the possible outcomes. The resulting state is again a product state of the two data qubit-state and the computational two ancilla state corresponding to the measurement result. In other words, data-qubits and ancillas are disentangled and therefore a two-data qubit state can once more be identified. Its coefficients, however, do not depend linearly on the initial amplitudes. Therefore, the change cannot be interpreted as a unitary data-qubit gate. This is due to the projective measurement of the ancillas. As we have seen, such an interpretation is valid for a measurement with probability one.

Another observation concerning the gate construction is the necessity of the ancillas being initialized in one of the computational states. If the initial state of the ancillas is a superposition, we cannot identify an instant of time where a specific measurement result is certain. Once more, this prohibits a unitary two-data qubit gate interpretation.

VI. CONCLUSION

Four electron spin qubits in quantum dots subject to a magnetic field have been modelled by a standard exchange Hamiltonian. Two data qubits and two ancilla qubits are considered; the exchange interaction is only present between a data-qubit and an ancilla. The time-independent symmetric case is solved by constructing the eigenbasis of the Hamiltonian and computing the corresponding energy eigenvalues.

As an application, the resulting evolution operator is exploited to obtain the time evolution of selected states. These states are product states of data-qubit Bell states and specific ancilla basis states. They are known to be the stable output states of the X and Z stabilizing circuit [9]. Unitary evolution of the stable states before the measurement of the ancillas is calculated. Resulting probabilities for the error syndrome and fidelities can be obtained. They are seen to differ substantially from the non-evolving case. As extensively discussed in [10], it may lead to reconsideration of the proposed error correction and surface codes for fault-tolerant computation.

The present study, however, indicates that this possible problem is less serious for electron spin qubits than for superconducting qubits coupled to resonators considered in [10]. We have shown for the considered model that Hamiltonian unitary evolution scales with the exchange coupling. Hence, it suggests to tune down the exchange interaction in the idle periods of time, *i.e.*, if it is not required. For coupling $\mathcal{J} = 800$ MHz, we have obtained a typical time interval of 4 ns for probabilities to change from zero to one and vice versa. Decreasing the coupling to $\mathcal{J} \approx 200$ kHz, a realistic minimum value [13], yields for that time interval $16\mu\text{s}$, which excludes unwanted rapid changes in probabilities and fidelities.

The possibility of verifiable two-qubit phase gates due to unitary evolution is shown. The verification is done by means of ancilla measurement. After the prescribed elapsed evolution time, the probabilities for finding the respective ancilla measurement results are one and zero. Consequently, obtaining the correct measurement result confirms the realization of the two-qubit operation without disturbing the final data-qubit state. An explicit decomposition of the found phase gate in terms of a CNOT and controlled single qubit rotations is given. It can also be written as product of two single qubit rotations and is therefore no alternative for controlled two-qubit operations in quantum computing.

Nevertheless, the verifiable two-qubit gate may have some benefits as its verifiability. Furthermore, the uni-

tary gate governed by Hamiltonian evolution is equivalent to *two* single qubit operations induced by microwave pulses. These possible merits have to be assessed in future experiments with electron spin devices.

Large scale fault-tolerant quantum computation is the long-term goal of ongoing research for developing quantum computers using various qubits. The considered four electron spin qubit system may be used as building block, or unit cell, in such an extended electron spin quantum device. Of course, these unit cells need to be eventually coupled by, for example, electromagnetic resonators. The symmetry of the unit cells, characterized by their total spin, appears to be advantageous for analyzing such possible developments.

ACKNOWLEDGMENTS

The author would like to thank G.J.N. Alberts, A.-J. de Jong, T. Last, L.M.K. Vandersypen and R. Versluis for stimulating discussions and/or a critical reading of the manuscript. This research is supported by the Early Research Programme of the Netherlands Organisation for Applied Scientific Research (TNO). Additional support from the Top Sector High Tech Systems and Materials is highly appreciated.

-
- [1] H.-A. Engel, L.P. Kouwenhoven, D. Loss, and C.M. Marcus, *Spins in few-electron quantum dots*, Quant. Infor. Proc. **3**, 115 (2004).
 - [2] R. Hanson, L.P. Kouwenhoven, J.R. Petta, S. Tarucha and L.M.K. Vandersypen, *Spins in few-electron quantum dots*, Rev. Mod. Phys. **79**, 1217 (2007).
 - [3] E. Kawamaki, *Characterization of an electron spin qubit in a Si/SiGe quantum dot*, Ph. D. thesis, TUDelft (2016).
 - [4] D. Loss and D.P. DiVincenzo, *Quantum computation with quantum dots*, Phys. Rev. A **57**, 120 (1998).
 - [5] D. Loss, G. Burkard and D.P. DiVincenzo, *Electron spins in quantum dots as quantum bits*, Journal of Nanoparticle Research **2**, 401 (2000).
 - [6] N.W. Ashcroft and N.D. Mermin, *Solid State Physics*, International Edition, Saunders College HRW (1976).
 - [7] T. Meunier, V.E. Calado and L.M.K. Vandersypen, *Efficient controlled-phase gate for single-spin qubits in quantum dots*, Phys. Rev. B **83**, 121403(R) (2011).
 - [8] T.F. Watson *et al.*, *A programmable two-qubit quantum processor in silicon*, Letter Nature **555**, 633 (2018).
 - [9] A.G. Fowler, M. Mariantoni, J.M. Martinis, and A.N. Cleland, *Surface codes: Towards practical large-scale quantum computation*, Phys. Rev. A **86**, 032324 (2012).
 - [10] H.W.L. Naus and R. Versluis, *Consequences of unitary evolution of coupled qubit-resonator systems for stabilizing circuits in surface codes* arXiv:1811.09832 [quant-ph] (2018).
 - [11] C. Cohen-Tannoudji, B. Diu, F. Laloë, *Quantum Mechanics*, Volume **2**, Hermann, Paris, and Wiley-VCH (2005).
 - [12] M.A. Nielsen and I.L. Chuang, *Quantum Computation and Quantum Information*, Cambridge University Press, Cambridge, UK (2000).
 - [13] L.M.K. Vandersypen, *private communication*.